Characterization of a room temperature terahertz detector based on a GaN/AlGaN HEMT*

Zhou Yu(周宇), Sun Jiandong(孙建东), Sun Yunfei(孙云飞), Zhang Zhipeng(张志鹏),
Lin Wenkui(林文魁), Liu Hongxin(刘宏欣), Zeng Chunhong(曾春红), Lu Min(陆敏),
Cai Yong(蔡勇), Wu Dongmin(吴东岷), Lou Shitao(楼柿涛), Qin Hua(秦华)†,
and Zhang Baoshun(张宝顺)

Key Laboratory of Nanodevices, Suzhou Institute of Nano-Tech and Nano-Bionics, Chinese Academy of Sciences,
Suzhou 215123, China

Abstract: We report on the characterization of a room temperature terahertz detector based on a GaN/AlGaN high electron mobility transistor integrated with three patch antennas. Experimental results prove that both horizontal and perpendicular electric fields are induced in the electron channel. A photocurrent is generated when the electron channel is strongly modulated by the gate voltage. Despite the large channel length and gate-source/drain distance, significant horizontal and perpendicular fields are achieved. The device is well described by the self-mixing of terahertz fields in the electron channel. The noise-equivalent power and responsivity are estimated to be $100\ \mathrm{nW}/\sqrt{\mathrm{Hz}}$ and 3 mA/W at 292 K, respectively. No decrease in responsivity is observed up to a modulation frequency of 5 kHz. The detector performance can be further improved by engineering the source-gate-drain geometry to enhance the nonlinearity.

Key words: terahertz detector; high electron mobility transistor; mixing; two-dimensional electron gas
DOI: 10.1088/1674-4926/32/6/064005   **PACC:** 7220J; 7340Q

1. Introduction

Compared to the relatively slow detectors that are based on calorimetric or bolometric effects, such as pyroelectric (PE) detectors and silicon bolometers, solid-state terahertz (THz) electromagnetic radiation detectors that operate at room temperature may offer both high sensitivity and high speed. Such superior characteristics are paramount for realising practical THz receivers for imaging, communication and radar applications[1]. One candidate is the direct-sensing Schottky diode already widely used in radio-frequency, microwave and optoelectronics. However, Schottky diodes that operate at THz frequencies require advanced materials and nano fabrication techniques to realize both ultra-low electron transit times and (parasitic) capacitance. In the past decade, THz detectors based on solid-state plasmon have been proposed and demonstrated both at cryogenic and room temperatures[2−13]. These plasmonic devices utilize the resonance between high density two dimensional[2,4,6] or three dimensional[7] electron gas and the incident THz wave. Due to their resonant nature, plasmonic detectors offer high sensitivity and possibly the ability to resolve the spectrum. However, further progress in plasmonic THz optoelectronic devices is still limited by the lack of a breakthrough in manipulating the interplay of plasmon resonance and electrical transport[7,8]. Recently, subterahertz detectors and focal plane arrays based on complementary metal–oxide–semiconductor (CMOS) technology have been

developed for operation at room temperature[14−16]. A self-mixing model based on the resistive network of the field-effect transistor is found to be adequate for analyzing devices operating in the non-resonant detection regime. Here, we report THz detection by a modified GaN/AlGaN high-electron-mobility transistor (HEMT), in which three THz patch antennas are engineered in a way so that THz radiation is effectively coupled to the source, drain and gate electrodes. An attempt to find the physical origin of terahertz photocurrent is described and we verify that the device operates as a mixer around 1 THz.

2. Device fabrication and experimental setup

The HEMT device is fabricated from a GaN/ $\mathrm{Al_{0.27}Ga_{0.73}N}$ heterostructure, which provides a two-dimensional electron gas (2DEG) about 23 nm below the surface. The 2DEG has an electron mobility of 1400 $\mathrm{cm^2/(V \cdot s)}$ and an electron density of 1.3×10^{13} $\mathrm{cm^{-2}}$ at room temperature. An electron channel is formed from the 2DEG by UV lithograph and has a length of 8 μm and a width of 10 μm. In between the source and drain electrodes, a Schottky gate with a length of 2 μm controls the electron channel. The distance between gate and source/drain is 3 μm. In order to guide THz radiation into the active area, the source, drain and gate electrodes are extended to three THz patch antennas (100 μm × 100 μm). Figure 1(a) is a scanning electron microscope (SEM) micrograph of the device. Upon
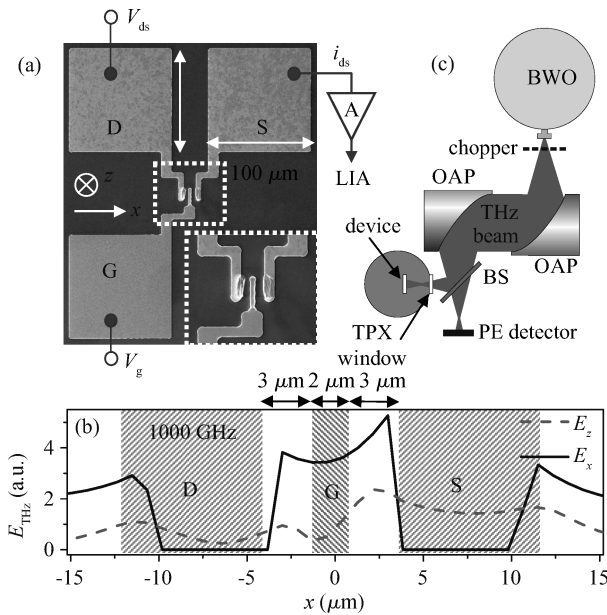
Fig. 1. (a) The SEM micrograph of a GaN/AlGaN HEMT device. (b) An electromagnetic simulation reveals the electric field distribution (E_x and E_z) in the electron channel (23 nm below the gate). (c) Schematics of the measurement setup.

THz irradiation at 1 THz, both electric fields along and perpendicular to the electron channel are induced under the gate, which is confirmed by finite-difference-time-domain (FDTD) simulation, as shown in Fig. 1(b). The setup for characterizing the device is shown in Fig. 1(c), where the THz radiation from a backward wave oscillator (BWO) is chopped, collected, collimated and focused onto the HEMT device located in a liquid nitrogen dewar. As the detector is insensitive to visible light, a 5 mm thick Polymethylpentene (TPX) disk is used as the window. For calibration, the THz beam is split ($T/R \approx 0.96$) by a high resistivity silicon wafer (BS) and guided to a PE detector (Model SPI-A-62THZ from the Spectrum Detector Inc.). Depending on the spot size, the ratio of the THz power density on the HEMT detector and on the PE detector is about 0.4. The source current is amplified by a DL1211 current preamplifier and a following lock-in amplifier (LIA). The drain–source bias (V_{ds}) is fixed at around 100 μV to maintain a minimal background source current less than 10 pA.

3. Results and discussion

As shown in Fig. 2(a), the differential conductance $G = \mathrm{d}I_{ds}/\mathrm{d}V_{ds}$ as a function of the gate voltage (V_g) is characterized at 77 K. Without THz radiation, the 2DEG under the gate can be pinched off completely at $V_g \leqslant -4.8$ V and fully opened when $V_g \geqslant -3.8$ V. Under THz irradiation at 1027 GHz, a direct photocurrent (i_{ds}) is induced when the electron channel is strongly modulated by the gate voltage, as shown in Fig. 2(b). The photocurrent dies out when the electron channel is completely pinched off. The peak photocurrent response is located at $V_g = -4.474$ V which is independent on the THz frequency, indicating a non-resonant detection mechanism[4]. With THz radiation, the pinch-off voltage is lowered by about 0.3 V,
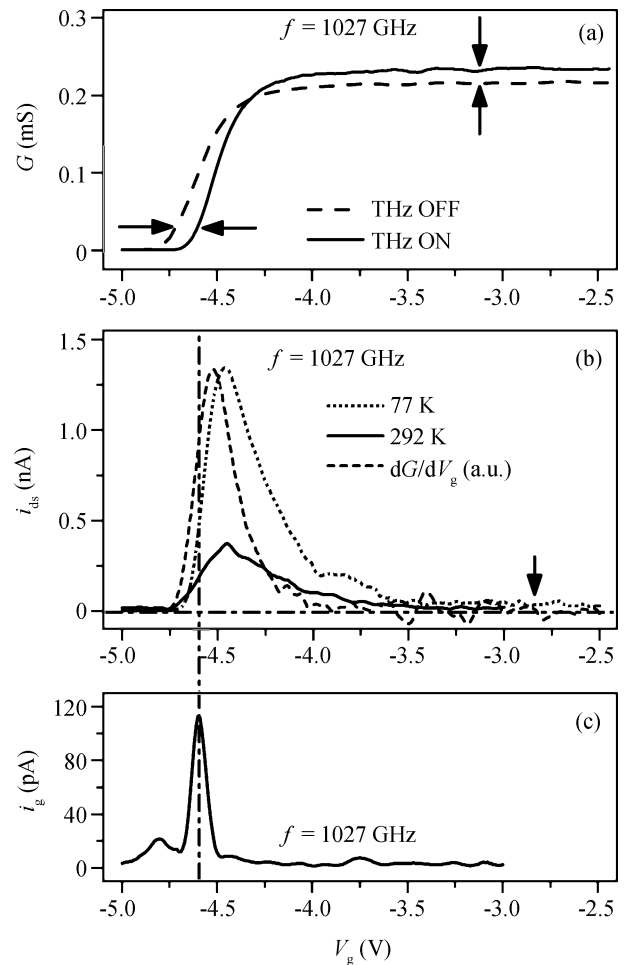
Fig. 2. (a) The channel conductance modulated by the gate voltage. (b) The drain–source photocurrent. (c) The photocurrent through the gate.

which is mainly from the charge storage between the gate and the electron channel causing hysteresis when the gate voltage is swept back and forth. A slight increase in conductance is clearly induced by THz irradiation, as shown in Fig. 2(a). We believe the increase in conductance is in connected to the weak photocurrent when the electron channel is fully open (open state, indicated by the vertical arrow in Fig. 2(a) and 2(b). The open-state photocurrent has two possible origins: (1) THz rectification by imperfect ohmic contacts at the source and drain, and (2) asymmetric travelling longitudinal electric field accompanying the plasma wave. However, the above two effects are indistinguishable in the current device structure. Nevertheless, it is clear that a finite horizontal THz electric field is induced between the source and drain contacts, as has been predicted by the FDTD simulations.

Apart from the source photocurrent, we also observe photocurrent ($\leqslant$ 120 pA) in the gate electrode, as shown in Fig. 2(c). However, it is about one order of magnitude smaller than the source photocurrent. The peak response around -4.61 V is about 0.15 V away from the peak in source photocurrent. A calculation shows that such a weak current induces a shift of only a few millivolts in the gate voltage. Hence, the gate current is irrelevant to the observed large source photocurrent. In fact, even without THz radiation, a gate leakage

current is observed among the devices we fabricated. The leakage current stems from electron tunneling through the Schottky barrier under the gate. We found that a leakage current below 10 nA does not affect device performance. The existence of a photocurrent through the gate is direct evidence that the THz radiation is coupled to the gate electrode and a perpendicular electric field is induced.

Based on the above experimental and simulation facts that both a horizontal and a perpendicular electric fields are induced in the electron channel, the validation of a self-mixing model is examined[4, 15]. Suppose $\delta \tilde{V}_g = \delta V_g \cos \omega t$ and $\delta \tilde{V}_{ds} = \delta V_{ds} \cos(\omega t + \phi)$ are the electric potentials induced in the electron channel under the gate. The THz frequency is referred as ω and ϕ is the phase shift between the potentials. Since V_{ds} is fixed around zero, the total source current under THz radiation is determined by $I_{ds} = G(V_g + \delta \tilde{V}_g)(V_{ds} + \delta \tilde{V}_{ds})$. Due to the fact that $\delta \tilde{V}_g \ll V_g$, the conductance term can be rewritten as $G(V_g) + \delta \tilde{V}_g dG(V_g)/dV_g$. Thus the photocurrent becomes $i_{ds} = \delta V_g \delta V_{ds} \cos \phi \dot{G}(V_g)/2 \propto \dot{G}(V_g) P_{THz}$, where P_{THz} is the incident THz power and $\dot{G}(V_g) = dG/dV_g$. It is then an engineering challenge to increase the field product and the derivative of channel conductance as large as possible at the same location in the electron channel. As shown in Fig. 2(b), the derivative of the conductance is compared to the photocurrent. Apart from the similarity in overall gate-voltage dependence, a difference in peak position and width are readily seen. The deviations may stem from two factors: (1) non-uniform electric fields induced under the gate (as shown in Fig. 1(b)), (2) finite series resistance of the ohmic contacts. It is noticeable that the self-mixing model can not explain the non-zero open-state photocurrent since the derivative of the channel conductance vanishes when the channel is fully open. In principle, it is possible that a travelling longitudinal plasma wave excited by the gate can produce a directional photocurrent, whose polarity is determined by unbalanced transmission to the drain and source contacts. However, a phase difference ϕ can induce a signal change as well. In order to reveal the profound nature of a THz photocurrent, a specially designed device will be fabricated and tuned to manipulate the polarity of photocurrent.

Due to a decrease in electron mobility at higher temperatures, the detector operating at 292 K has a lower sensitivity (30%) and a larger background noise compared to that at 77 K, as shown in Fig. 2(b). We directly compare the detector biased at its optimal operating point ($V_{ds} = 100 \, \mu V$, $V_g = -4.474$ V) to the PE detector. The PE detector is a broadband detector with a responsivity of 150 kV/W, hence its output signal represents the THz power from the BWO source. In Fig. 3(a), the detector responses at 1027 GHz are compared when the THz radiation is attenuated step by step. The linear relation indicates that the HEMT detector is a good power meter for THz radiation measurement. The current responsivity is estimated to be about 3 mA/W at 292 K and 9 mA/W at 77 K. From the measured background current and the bandwidth of the lock-in amplifier, we estimated the noise equivalent power (NEP) to be about 100 nW/$\sqrt{\text{Hz}}$ at 292 K and below 10 nW/$\sqrt{\text{Hz}}$ at 77 K, respectively. It is clear that the background current noise mainly comes from thermal fluctuations in the electron channel. By increasing the channel width, the NEP could be reduced without affecting the responsivity. Furthermore, a shorter elec-
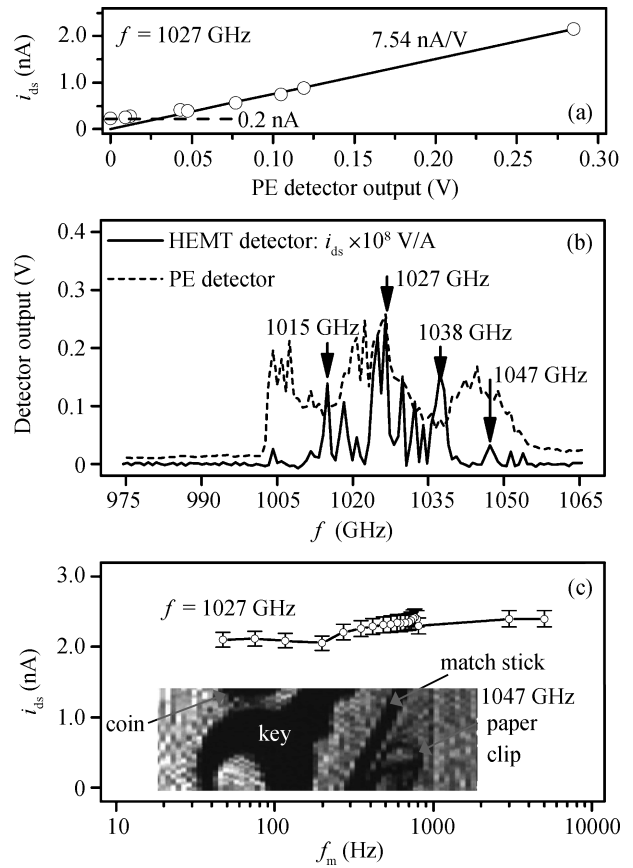
Fig. 3. (a) The linear power response at $f = 1027$ GHz. (b) The frequency response. (c) The response time at $f = 1027$ GHz. Inset: raster-scan image taken at 1047 GHz and at a modulation frequency of 706 Hz. All data are taken at 292 K.

tron channel will allow for both higher sensitivity and a lower NEP.

The detector's spectral response is examined by sweeping the BWO frequency from 960 GHz to 1088 GHz in a step of 12.8 GHz, as shown in Fig. 3(b). At 1038 GHz, the device shows enhanced sensitivity. Sensitive detection can be realized at other frequencies, such as 1015, 1027, and 1047 GHz. Unlike the broadband PE detector, such frequency selectivity is a nature of patch antennas. However, detectors based on self-mixing have a much higher speed, which is limited by the RC time constant ($\lesssim 10$ ns) of the electron channel. As shown in Fig. 3(c), no decrease in sensitivity is observed up to 5 kHz, which is the highest modulation frequency accessible with the electromechanical chopper. Operating the HEMT device as a single pixel detector at room temperature, a raster scan of a focused THz beam over a sealed envelope is performed with a modulation frequency of 706 Hz. As shown in the inset of Fig. 3(c), the image clearly reveals the objects sealed in the envelope. The THz frequency is chosen to be 1047 GHz so that the imaging quality is examined when the detector offers a low sensitivity of only 0.3 mA/W. At frequencies with higher responsivity, the imaging quality is considerably enhanced.

4. Conclusion

In conclusion, a compact THz detector based on a

GaN/AlGaN HEMT is fabricated and characterized in the frequency range from 1000 GHz to 1055 GHz at 77 K and at room temperature. THz radiation is coupled effectively into the electron channel by three antennas and generates a strong source-drain photocurrent. No shift in the photocurrent peak is observed at different frequencies and the bandwidth of this non-resonant detection is determined by the antennas. The self-mixing model is in good agreement with the experimental results.

The detector responsivity is in the same order of magnitude as those reported in reference[16]. However, our detector has a micron-sized electron channel whereas the electron channels in other detectors were controlled by nanometer-sized gates[10−16]. Despite the fact that the longer channel reduces transconductance and increases detector resistance, the overall detector performance is elevated by our integrated patch antennas, which enhance the product of the perpendicular and horizontal THz electric fields. By reducing the channel length down to nanometer scale, the detector performance can be further improved. A two dimensional electron gas (2DEG) in GaN/AlGaN offers higher electron mobility and a much higher electron density than that in a silicon-based CMOS device. Although GaAs/AlGaAs offers even higher electron mobility, strong absorption of the terahertz wave by the GaAs substrate may cause tremendous difficulties in realizing a focal plane array where the THz light has to be guided through the substrate to the detectors. Instead, GaN/AlGaN is usually grown on sapphire which is highly transparent for terahertz waves.

Our detector in a three-terminal nature is operated with zero source–drain bias which minimizes the shot noise. In such an operation mode, readout circuits for infrared imaging can be adopted. A room temperature detector and focal plane array with higher sensitivity and higher speed can be realized. New devices including deliberately engineered gates are in fabrication and will be examined to manipulate the plasmonic and electronic interactions.

References

[1] Tonouchi M. Cutting-edge terahertz technology. Nature Photonics, 2007, 1: 97

[2] Shaner E A, Grine A D, Wanke M C. Far-infrared spectrum analysis using plasmon modes in a quantum-well transistor. IEEE Photonics Technology Letters, 2006, 18: 1925

[3] Dyakonov M, Shur M S. Detection, mixing, and frequency multiplication of terahertz radiation by two-dimensional electronic fluid. IEEE Trans Electron Devices, 1996, 43: 380

[4] Satou A, Ryzhii V, Mitin V. Damping of plasma waves in two-dimensional electron systems due to contacts. Phys Status Solidi, 2009, 9: 2146

[5] Knap W, Dyakonov M, Coquillat D. Field effect transistor for terahertz detection: physics and first imaging applications. J Infrared Milli Terahz Waves, 2009, 30: 1319

[6] Stillman W J, Shur M S. Closing the gap: plasma wave electronic terahertz detectors. Journal of Nanoelectronics and Optoelectronics, 2007, 2: 209

[7] Kim S, Zimmerman J D. Room temperature terahertz detection based on bulk plasmons in antenna-coupled GaAs field effect transistors. Appl Phys Lett, 2008, 92: 253508

[8] Fatimy A El, Tombet S B, Teppe F. Terahertz detection by GaN/AlGaN transistors. Electronics Letters, 2006, 42:1342

[9] Tauk R, Teppe F, Boubanga S. Plasma wave detection of terahertz radiation by silicon field effects transistors: responsivity and noise equivalent power. Appl Phys Lett, 2006, 89: 253511

[10] Teppe F, Veksler D, Kachorovski V Y. Plasma wave resonant detection of femtosecond pulsed terahertz radiation by a nanometer field-effect transistor. Appl Phys Lett, 2005, 87: 022102

[11] Knap W, Teppe F, Meziani Y, et al. Plasma wave detection of subterahertz and terahertz radiation by silicon field-effect transistors. Appl Phys Lett, 2004, 85: 675

[12] Knap W, Kachorovskii V, Deng Y, et al. Nonresonant detection of terahertz radiation in field effect transistors. J Appl Phys, 2002, 91: 9346

[13] Knap W, Deng Y, Rumyantsev S, et al. Resonant detection of subterahertz and terahertz radiation by plasma waves in submicron field-effect transistors. Appl Phys Lett, 2002, 81: 4637

[14] Glaab D, Boppel S, Lisauskas A. Terahertz heterodyne detection with silicon field-effect transistors. Appl Phys Lett, 2010, 96: 042106

[15] Lisauskas A, Pfeiffer U R, Öjefors E. Rational design of high-responsivity detectors of terahertz radiation based on distributed self-mixing in silicon field-effect transistors. J Appl Phys, 2009, 105: 114511

[16] Öjefors E, Lisauskas A, Glaab D. Terahertz imaging detectors in CMOS technology. J Infrared Milli Terahz Waves, 2009, 30: 1269